Electrical Power and Energy Systems 148 (2023) 108999

Contents lists available at ScienceDirect

International Journal of Electrical Power and Energy Systems

journal homepage: www.elsevier.com/locate/ijepes

A stochastic distributed control approach for load restoration of networked microgrids with mobile energy storage systems

Y. Wang, A. Oulis Rousis, D. Qiu *, G. Strbac

Department of Electrical and Electronic Engineering, Imperial College, London, UK

ARTICLE INFO

Keywords:
Resilience
Networked MGs
Mobile energy storage systems
Distributed control
Rolling optimization
AC OPF

ABSTRACT

In response to extreme events, substantial research efforts have focused on developing load restoration strategies for networked microgrids (MGs). However, existing distributed control approaches only consider independent time periods, which cannot capture the time-coupled flexibility of storage units. Additionally, mobile energy storage systems (MESSs) have been deployed for resilience enhancement due to their advantages in mobility and flexibility. However, existing research on networked MGs utilizes simplistic energy management approaches for MG modeling without detailed network structures, which cannot capture the mobility of MESSs. To address these issues, this paper proposes a three-stage stochastic distributed control approach based on rolling optimization to enhance the resilience of networked MGs with MESSs. Specifically, a stochastic linearized OPF is formulated in the first stage to capture the flexibility of MESSs and uncertainties, while a consensus algorithm is utilized in the second stage to calculate the power exchange among MGs. Finally, a detailed non-linear AC OPF algorithm is employed in the third stage to capture technical constraints relating to stability properties towards accurate optimization results. Case studies considering load distinction, multiple line outages, and limited generation resources are developed to demonstrate the effectiveness of the proposed distributed control approach in accurate and timely decision-making.

1. Introduction

Extreme weather events including natural disasters (e.g., hurricanes, storms, etc.) and man-made events (e.g., cyber or physical attacks) are featured by high impact and low probability (HILP), which can affect the status of components in power systems (e.g., power plants, substations, and cables) and cause severe power outages [1]. Recently, the significantly increasing penetration of renewable energy resources (RESs) has been witnessed in power systems, where their intermittent and fluctuating nature further exacerbates the impact of extreme events. To deal with these HILP events, the concept of 'resilience' is introduced in power systems [2]. Given the serious disruptions, the main goal of a resilient power system should be to maintain the supply continuity of essential loads (e.g., medical facilities and police stations), constituting a system load restoration problem [3].

In this context, microgrids (MGs), as localized small power systems with enhanced control capabilities, are regarded as an effective solution to integrate and coordinate different types of distributed energy resources (DERs) (e.g., diesel generators (DGs), RESs, energy storage systems (EESs), etc.) for resilience enhancement [4]. It can be anticipated that small-scale MGs will become common in the coming decades and play a crucial role in the development of future energy systems worldwide due to the essential benefits they provide for resilience enhancement in decentralized operating paradigms [5]. Specifically, several MGs can even connect with each other as an MG cluster, where the power sharing among these MGs can effectively increase the survivability of essential loads during extreme events [6]. On the other hand, as an emerging type of DERs, mobile energy storage systems (MESSs) have been gradually deployed in current power systems for resilience enhancement due to their significant advantages on mobility and flexibility compared to static ESSs [7]. In this context, instead of integrating static ESSs, MGs can choose to involve MESSs for system load restoration towards a higher resilience level. As such, this paper aims to develop a stochastic distributed control approach based on rolling optimization for the resilience-oriented routing and scheduling of MESSs in networked MGs towards load restoration after extreme events, which is generic enough to handle main contingencies caused by both natural and man-made events.

* Correspondence to: Department of Electrical and Electronic Engineering, South Kensington Campus, London, SW7 2AZ, UK.
E-mail address: d.qiu15@imperial.ac.uk (D. Qiu).
URL: https://scholar.google.com/citations?user=H9zHATgAAAAJ&hl=zh-CN&oi=ao (A.O. Rousis).

https://doi.org/10.1016/j.ijepes.2023.108999
Received 30 September 2022; Received in revised form 14 November 2022; Accepted 24 January 2023
Available online 31 January 2023

Nomenclature

Parameters

Δt	Time interval
η^c	Efficiency of storage device(s) during charging
η^d	Efficiency of storage device(s) during discharging
B_{bp}	Susceptance of branch connecting AC buses b, p
G_{bp}	Conductance of branch connecting AC buses b, p
c_b^{ls}	Cost associated with load shedding of bus b
c^e	Penalty coefficient associated with power surplus/shortage
ES_k^{max}	Maximum state of charge in MESS k
ES_k^{min}	Maximum depth of discharge in MESS k
GS_g^{Ini}	Initial generation resource state of generator g
GS_g^{min}	Minimum energy reserve of generator g
P_g^{max}	Maximum active power of generator g
P_g^{min}	Minimum active power of generator g
Q_g^{max}	Maximum reactive power of generator g
Q_g^{min}	Minimum reactive power of generator g
P_k^{max}	Maximum storage power of MESS k
T	Time scheduling horizon
T_{ij}^{max}	Tie-line capacity between MG i and MG j
V^{max}	Maximum permissible voltage
V^{min}	Minimum permissible voltage
$D_{b,p}$	The traveling time of MESS k from bus b to bus p

Sets

G_{bus}	Total number of generator buses, $G_{bus} \subset N_{bus}$
L_{bus}	Total number of load buses, $L_{bus} \subset N_{bus}$
N_{br}	Total number of branches
N_{bus}	Total number of buses
N_g	Total number of generators in an MG
N_{mes}	Total number of MESSs
M	Total number of connected MGs in the MG cluster

Variables

$\delta_{b,t,s}$	Voltage angle of bus b at time step t under scenario s
$\delta_{bp,t,s}$	Voltage angle difference between buses b, p at time step t under scenario s
$GS_{g,t,s}$	Energy reserve of generator g in an MG at the end of time step t under scenario s
$P_{g,t,s}$	Active power generation of generator g at time step t under scenario s
$P_{b,t,s}^{ex}$	Active power exchange between considered bus b and other buses at time step t under scenario s
$P_{b,t,s}^{ls}$	Involuntary loss of active load at bus b at time step t under scenario s
$P_{b,t,s}^{l}$	Active load at bus b at time step t under scenario s
$Q_{g,t,s}$	Reactive power generation of generator g at time step t under scenario s
$Q_{b,t,s}^{es}$	Reactive power exchange between considered bus b and other buses at time step t under scenario s
$Q_{b,t,s}^{ls}$	Involuntary loss of reactive load at bus b at time step t under scenario s
$Q_{b,t,s}^{l}$	Reactive load at bus b at time step t under scenario s
$P_{bp,t,s}$	Active power flow of branch bp at time step t under scenario s
$Q_{bp,t,s}$	Reactive power flow of branch bp at time step t under scenario s
$V_{b,t,s}$	Voltage at bus b at time step t under scenario s
$u_{b,k,t}$	Integer variable that shows the status of MESS k in bus b at time step t
$P_{b,k,t}^{mes,c}$	Charging of MESS k into bus b at time step t
$P_{b,k,t}^{mes,d}$	Discharging of MESS k into bus b at time step t
$ES_{k,t}$	Energy content of MESS k at time step t
P_t^e	Power shortage/surplus at time step t
$P_{i,t}^{sur}$	Power surplus of MG i at time step t
$P_{i,t}^{sho}$	Power shortage of MG i at time step t
$P_{i,t}^{ob}$	The power obtained from connected MGs in MG i at time step t

1.1. Literature review on networked MGs and MESSs

Recently, much research has focused on the benefits of networked MGs on resilience enhancement, where centralized control, hierarchical control, and distributed control are three basic approaches to operate these MGs [4]. Planning and operation strategies based on centralized control have been widely developed to enhance the resilience of networked MGs [8–11], since this research area has been a lot more mature. For instance, in [8], the resilience-oriented coordination between EESs, mobile power resources, and network reconfiguration is investigated to enhance the resiliency of networked MGs. In [9], a two-stage stochastic optimization program based on a decomposition algorithm is proposed to operate networked MGs towards resilient distribution grids. In [10], a comprehensive operation and self-healing strategy is developed to optimally formulate networked self-supplied MGs against power outages. In [11], a risk-constrained adaptive robust optimization approach is proposed to provide proactive resilient scheduling decisions for networked MGs during extreme events. However, it is worth noting that MG operations based on centralized control approaches can become extremely time-consuming with the increase in the number of connected MGs. The highly uncertain nature of extreme events may not allow the central controller to make decisions in time. Additionally, the requirement of centralized control for high information sharing among MGs may introduce security problems. To address this issue, hierarchical control schemes are developed in [12–15], which can largely reduce the computing burden of central controllers and the information that needs to be shared among MGs. However, this control approach still requires a central controller to manage local MGs, which can be prone to a single-point failure.

In comparison with centralized control, distributed control approaches may not guarantee a globally optimal solution but can protect customer privacy and reduce the dependency of networked MGs on communication networks [16]. Recently, there has been much research focused on developing distributed operation strategies for the resilience enhancement of networked MGs. In [17], a decentralized collaborative dispatch framework based on consensus algorithm is proposed for the effective power exchange of networked MGs. In [18], an nested energy management strategy is developed for the day-ahead scheduling of networked MGs, which considers both grid-connected and islanded modes of MGs. However, no uncertainties are considered in the above two papers. In [19], a peer-to-peer energy bartering framework based on a consensus algorithm is developed for power sharing between interconnected MGs, while ignoring the influence of uncertainties on optimization results. In [20], a decentralized operation model including buying/selling power, charging/discharging of ESSs, and demand

response is developed for multiple cooperative MGs. Uncertainties of RESs are addressed in MG operations via a two-stage adjustable robust optimization approach. In [21], a distributed control approach based on the alternating direction method of multipliers is suggested to manage the power sharing between MGs and distribution networks, where uncertainties with market price are captured via robust optimization. In [22], a distributed control scheme considering feasible islanding in normal mode and load survivability in emergency mode is developed for the resilience enhancement of networked MGs, where an incremental cost consensus algorithm is employed for the power sharing between MGs. Uncertainties associated with RESs and loads are handled via robust optimization. However, this paper assumes a two-hour scheduling horizon for emergency cases, which may be unrealistic.

Going further, it is worth noting that the aforementioned papers utilize energy management systems (EMSs) to model MG operations, which can only capture the power balance equations of an MG model. Given the absence of detailed constraints for the MG network topology, it is impossible to use EMSs to model the spatial flexibilities of MESSs. Note that MESSs can introduce significant merits for resilience enhancement of power systems via delivering power and energy as backup power sources for load restoration [23]. For instance, in [24], the routing and scheduling characteristics of MESSs are incorporated with the dispatches of repair crews towards the load restoration of distribution systems. In [25], a temporal–spatial model capturing the routing process of MESSs and network reconfiguration is developed to minimize the total system cost (e.g., load shedding cost and generation cost). Furthermore, the absence of technical constraints relating to voltage, angle, and power losses can lead to unstable MG operations and inaccurate solutions during extreme events, since power systems will be operated much closer to their stability limits under high uncertainties and severe contingencies [26].

To address the above issues on the lack of detailed network models, MG network models are considered in [27–31] to simulate the realistic operation scenarios of networked MGs. For instance, in [27], a distributed control approach based on a two-layer communication protocol is proposed for the resilience-oriented operation of networked MGs. Both normal and self-healing operation modes are captured and the power exchange between MGs is achieved by a consensus algorithm; nevertheless, this paper assumes a deterministic framework without considering any uncertainties. In [28], a stochastic bi-level optimization model based on a linearized distflow algorithm is developed in [28] to coordinate the power exchange between MGs and the utility grid in a decentralized manner. The first level is used to conduct negotiations between different entities, while the second level is employed to update non-converging penalties. Uncertainties relating to RESs and load profiles are captured via stochastic programming. However, this paper does not consider the power sharing between MGs and the influence of severe contingencies on MG operation performance. Additionally, Ref. [28] does not consider a long emergency horizon but only system snapshots, which cannot capture the flexibility of storage systems (e.g., ESSs and MESSs). In [29], a coordinated power exchange mechanism based on distributed control is developed for load restoration after extreme events, while uncertainties relating to RESs and loads are considered using a Monte-Carlo simulation approach. In [30], an optimal scheduling strategy based on alternating direction method of multipliers is developed for networked MGs, while uncertainties associated with wind power are captured via robust optimization. In [31], a data-driven distributionally robust co-optimization model is proposed for the peer-to-peer energy trading and network operation of networked MGs, considering the uncertainties associated with RESs and loads. However, these papers utilize a linearized distflow algorithm for MG operations, which ignores voltage angle variations and power losses through lines and can only be applied in radial networks. It is worth noting that MGs may have different network structures, other than traditional distribution systems [32]. Meshed networks include a more uniform power flow and can provide benefits for improving voltage profiles and reducing power losses, which can introduce the strong capabilities of meshed networks to withstand severe contingencies and improve resilience [33].

1.2. Research gaps and contributions

To summarize, there have been a large number of studies focused on the resilience-oriented operation of networked MGs, including centralized control, hierarchical control, and distributed control. In general, both centralized control and hierarchical control approaches require central controllers for MG operations, which can be time-consuming and prone to single-point failure considering the high-impact and unpredictable nature of extreme events. To address these issues, distributed control approaches that do not require central controllers have attracted much research interest, where consensus-based algorithms are one of the main methods to achieve distributed control. Although many studies have demonstrated the benefits of distributed control approaches for the resilience enhancement of networked MGs, the following fundamental research gaps still remain:

- There has been much research on the distributed control of networked MGs; nevertheless, existing literature solves the optimization problem on an hourly basis or ignores long timeframes, which cannot capture the flexibility of storage units and power sharing between MGs. One of the reasons for this is that consensus-based algorithms found in the literature (e.g., [19,22,27,29]) address the power sharing between MGs in independent time periods, which are inherently unable to capture any time-coupled flexibility [34]. It is necessary to develop an optimization framework to comprehensively consider such flexibility under distributed control.
- Existing literature tends to utilize EMSs [17–22] or linearized distflow models [27–31] for MG operations due to the need of reducing the computing burden. There is little research focusing on control approaches, which can capture technical constraints relating to stability properties for accurate decision making and secure MG operations as well as ensuring computing efficiency.
- Compared with static DERs (e.g., ESSs), MESSs are capable of achieving more effective load restoration via their mobility and flexibility features, especially in the context of decentralization [23]. However, there is no significant amount of research focused on distributed control approaches capturing the merits of MESSs for the resilience enhancement of networked MGs.

To fill in the research gaps discussed above, this paper proposes a stochastic distributed control approach based on rolling optimization for the resilience-oriented operation of networked MGs with MESSs, which can effectively bridge a gap in this respective area. The contributions are summarized hereafter:

- A three-stage distributed control approach based on rolling optimization is developed for the resilience-oriented scheduling of networked MGs. A time-coupled linearized AC OPF algorithm is utilized in the first stage to capture the flexibility of storage units and uncertainties as well as ensuring computing efficiency.
- Time-coupled routing and scheduling characteristics of MESSs inside each MG are fully modeled for load restoration, while the transporting time of MESSs between different buses inside each MG is appropriately incorporated into the proposed model.
- A detailed one-step non-linear AC OPF algorithm is proposed in the third stage to capture stability properties relating to voltage, angle, and power losses to ensure accurate optimization results and no violation of technical constraints.

- Uncertainties with RESs and load profiles are captured in the first stage of the proposed model via a scenario-based stochastic programming approach. Multiple line outages, limited generation resources, and load distinction into critical and non-critical are included in the model to capture the main features of HILP events.

The remainder of the paper is organized as follows. Section 2 outlines the main challenges of HILP events and the suggested stochastic distributed control approach based on rolling optimization. Section 3 introduces the model formulation of networked MGs and MESSs in detail, followed by extensive case studies and discussion in Sections 4 and 5 respectively. Finally, in Section 6 conclusions are drawn.

2. Outline of the suggested resilience-oriented operation approach

In this paper, we focus on the resilience-oriented operation problem of a networked MG cluster involving MESS routing and scheduling characteristics towards the overall resilience enhancement. In general, when an event occurs, MGs may switch into islanded mode (from grid-connected mode) due to intentional or unintentional islanding schemes. To minimize the influence of the HILP event, these small-scale MGs can choose to connect with nearby MGs as a cluster via available communication resources, while they can do power sharing with each other in order to achieve a higher level of overall resilience considering the uncertainty of RESs and load profiles. Inside each MG, DERs, such as photovoltaics (PVs), diesel generators (DGs), and MESSs, are installed suitably, which can provide necessary power support for the MG.

2.1. Main challenges of HILP events and suggested solutions

As aforementioned, extreme events are characterized by high impact and low probability, which can potentially cause high uncertainties and severe damages to the MG cluster, including (1) islanded MGs losing their connection to the utility grid; (2) unavailable central controllers for MG cluster operations; (3) severe damages inside each MG (e.g., multiple line outages); (4) unavailable or limited generation resources; (5) uncertain event occurrence time and duration; (6) uncertain RESs and load profiles; (7) power system operations close to their stability limits.

Considering the aforementioned properties (1)–(2), the suggested control approach for networked MGs should be decentralized and flexible enough against extreme events [15]. In other words, MGs in the cluster shall operate within a distributed manner and have their own controllability without the central commands, which can avoid single-point failure and privacy concerns. To deal with the aforementioned issues (3)–(4), it is necessary to employ MESSs with enhanced flexibility and mobility for load restoration, since static energy resources may not be able to access interrupted loads due to the severe damage caused by extreme events. Regarding the above features (5)–(6) of extreme events, a rolling optimization approach can be applied to make timely scheduling decisions for these MGs, while a scenario-based stochastic programming approach can be introduced to capture the uncertain nature of RESs and load profiles. Finally, to reduce the risk of constraint violations caused by the above property (7), a detailed non-linear AC OPF algorithm is required to accurately capture all the technical constraints related to voltage, angle, power flow, and power losses for secure MG operations.

2.2. Stochastic distributed control within a rolling optimization framework

To address the aforementioned issues, this paper proposes a three-stage stochastic distributed control approach based on rolling optimization to capture realistic MESS routing and scheduling characteristics and make decisions on power exchange among MGs towards resilience enhancement, which is schematically represented by Fig. 1. Compared with centralized control (e.g., [8–11]), the proposed distributed control approach can be time-efficient and achieve timely

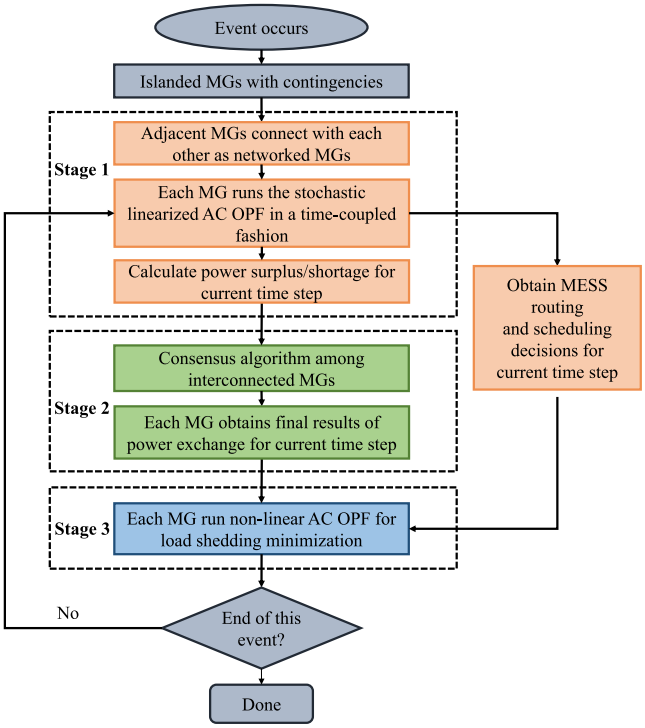

Fig. 1. Flowchart of the proposed three-stage distributed control approach based on rolling optimization.

critical load restoration. Compared with hierarchical control (e.g., [12–15]), the proposed distributed control approach can reduce the need for a central controller and avoid single-point failure. Compared with existing distributed control approaches (e.g., [19,22,27,29]), the proposed distributed control approach is incorporated with a detailed power network model and a rolling optimization framework, which can capture the time-coupled features of MESS routing and scheduling as well as power exchange. A more detailed description of the various elements at each stage can be found in Fig. 2.

According to Fig. 1, the proposed stochastic distributed control approach includes the following three stages:

- In the first stage, each MG schedules its local resources via a time-coupled stochastic linearized AC OPF algorithm, optimizing MESS routing and scheduling behaviors, calculating the power shortage and power surplus, and capturing uncertainties associated with RESs and load profiles. Only scheduling decisions on the current time step are utilized within the proposed rolling optimization framework. Specifically, the results of power shortage and power surplus of each MG are sent to the second stage, while the routing and scheduling decisions of MESSs are sent to the third stage.
- In the second stage, the results of power shortage or surplus received from the first stage are realized as the initialization of the consensus algorithm for distributed control. An iterative process is applied to obtain the final power exchange results among interconnected MGs that will be sent to the third stage for final verification.
- In the third stage, after receiving the final power exchange results and MESS routing and scheduling decisions, a deterministic non-linear AC OPF algorithm capturing stability properties is employed to ensure the feasibility of optimization results at the current time step, i.e., no violations of technical constraints.

Overall, these three stages are operated within the rolling optimization framework in an iterative manner until the event ends. It is worth noting that rolling optimization can optimize the system

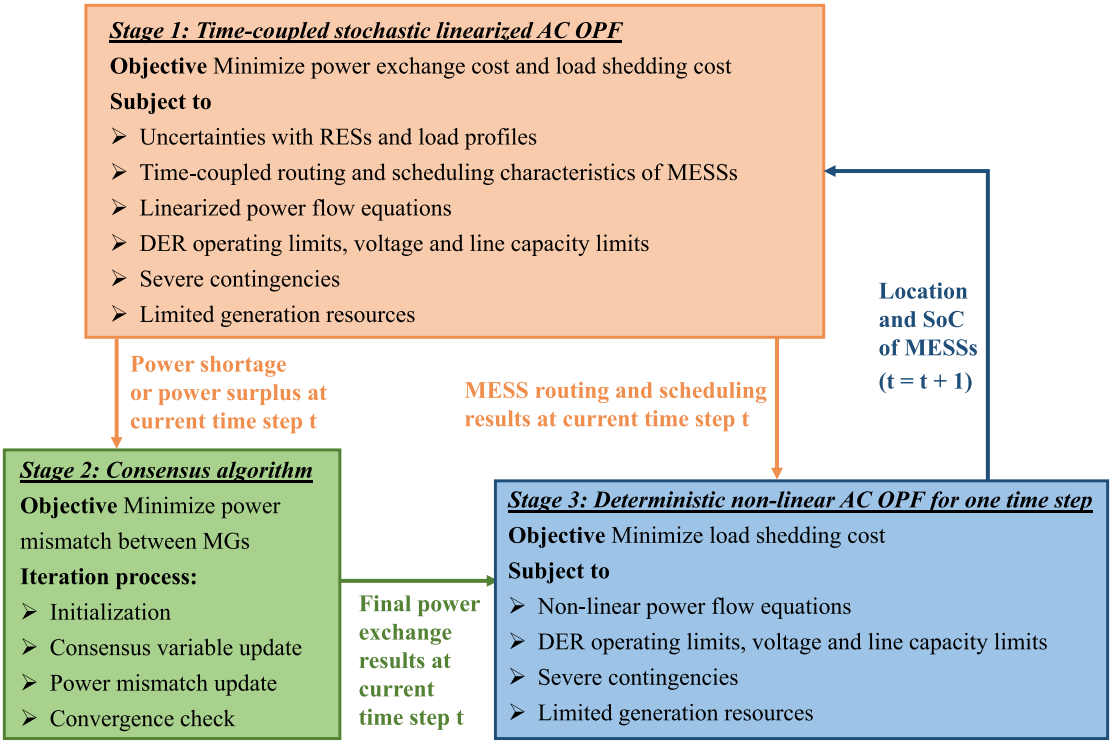

Fig. 2. Detailed information of each stage within the rolling optimization framework.

operation for the current time step while taking future time slots into account [15]. Detailed information about each stage can be found in Fig. 2, illustrating the objective functions and constraints (or iteration process) of these three stages.

Going further, it is worth noting that existing distributed control approaches based on consensus algorithms are inherently time-independent, which cannot effectively capture the flexibility of MESSs and power sharing in a time-coupled manner. However, the suggested stochastic distributed control approach provides the advantage of handling unforeseen changes and capturing the above flexibilities via the rolling optimization framework. Additionally, the influence of uncertain event time and duration on MG operations can be significantly reduced, since rolling optimization approaches are run on an hourly basis and have no dependence on the complete scheduling horizon. Furthermore, the computational burden is largely reduced due to the utilization of linearized AC OPF in the first stage, compared with the original non-linear AC OPF algorithm.

3. MG operation based on distributed control

As shown in Fig. 2, the suggested distributed control approach is divided into three distinct stages: (1) linearized stochastic AC OPF capturing time-coupled behaviors of MESSs and power sharing among MGs; (2) a consensus-based algorithm calculating power exchange for the current time step; (3) a detailed non-linear AC OPF utilized to obtain accurate optimization results and avoid the violation of technical constraints. Details of the proposed three-stage stochastic distributed control approach can be found hereafter:

3.1. Stage 1 — Calculate power surplus/shortage and obtain MESS routing and scheduling decisions

In the first stage, every MG runs a time-coupled linearized AC OPF algorithm in a stand-alone condition (i.e., not connected to other MGs) and calculates power shortage or power surplus (i.e., P_e) within the scheduling horizon. Note that only signals for one time step will be sent to the second stage to calculate the final results of power exchange. The objective function of one local MG in this stage can be found in (1). The first term corresponds to the real power surplus or power shortage, while the second term is related to the total load shedding cost capturing a set of uncertainties. In other words, the process of calculating power shortage/surplus for every MG is formulated as a scenario-based stochastic problem in which results are obtained according to a set of scenarios [35]. Variables on power shortage/surplus as well as the routing and scheduling of MESSs are realized as here-and-now decision variables, while the others (e.g., load shedding or power output of generators) are wait-and-see variables depending on the realization of each scenario.

$$F_1 = \sum_{t\in T} c^e P_t^e + \sum_{s\in S} p_s \sum_{t\in T} \sum_{b\in L_{bus}} c_b^{ls} P_{b,t,s}^{ls} \tag{1}$$

Incorporating typical non-linear technical constraints as well as MESS routing and scheduling constraints makes the model become a mixed-integer non-linear programming (MINLP) problem, which is extremely difficult to solve, especially with the consideration of time-coupled flexibilities and a set of uncertainties. In line with the requirements of resilience enhancement for computing efficiency, linearized techniques are required to simplify the non-linear OPF into a MILP formulation to obtain a trade-off between computing time and accuracy in the first stage [36]. As such, the optimization is posed as a minimization problem, subject to the following linearized AC OPF constraints (2)–(20). The active and reactive power balance equations at the exchange bus b are described in (2) and (3), respectively. Classical equations pertaining to power flow problems are presented in (4) and (5). $P_{b,t,s}^{ex}$ and $Q_{b,t,s}^{ex}$ represent active and reactive power exchange between considered bus b and other buses at time step t under scenario s respectively. $P_{b,k,t}^{mes,d}$ and $P_{b,k,t}^{mes,c}$ correspond to the power discharging and charging of MESS k on bus b at time step t. $P_{g,t,s}$ and $Q_{g,t,s}$ are the active and reactive power generation of DG g at time step t under scenario s. $P_{b,t,s}^{l}$ is related to the load level of bus b at time step t under scenario s. Constraints (6)–(7) refer to the network model, where $P_{bp,t,s}$ and $Q_{bp,t,s}$ are the active power and reactive power flow through the line from bus b to bus p.

$\delta_{bp,t,s}$ corresponds to the voltage angle difference between buses b and p at time step t under scenario s. P_{bp}^{L} and Q_{bp}^{L} correspond to active and reactive power losses, which can be linearized via the loss factors suggested by [36]. Eq. (8) corresponds to the power exchange limit between the MG i and nearby MG j, where T_{ij} refers to the tie-line capacity between MG i and MG j.

Furthermore, events may cause potential damage to energy supply chains, such as gas networks and fuel networks, and therefore generation resources (e.g., fuel reserve) within one MG may be limited [37]. In this context, it is reasonable to assume that each MG only has limited generation resources, which accounts for Eqs. (9) and (10). GS_{g}^{Ini} corresponds to the initial energy reserve of an MG when an event occurs and generator g will fail to operate when GS_{g}^{Ini} reaches its minimum value GS_{g}^{min}.

$$P_{t}^{e}+\sum_{k\in N_{mes}}(P_{b,k,t}^{mes,d}-P_{b,k,t}^{mes,c})+P_{b,t,s}^{ls}+\sum_{g\in NG_{b}}P_{g,t,s}=P_{b,t,s}^{ex}+P_{b,t,s}^{l} \tag{2}$$

$$\sum_{g\in NG_{b}}Q_{g,t,s}+Q_{b,t,s}^{ls}=Q_{b,t,s}^{ex}+Q_{b,t,s}^{l} \tag{3}$$

$$P_{b,t,s}^{ex}=\sum_{(b,p)\in N_{br}}P_{bp,t,s}+(\sum_{p\in N_{bus}}G_{bp})V_{b,t,s}^{2} \tag{4}$$

$$Q_{b,t,s}^{ex}=\sum_{(b,p)\in N_{br}}Q_{bp,t,s}-(\sum_{p\in N_{bus}}B_{bp})V_{b,t,s}^{2} \tag{5}$$

$$P_{bp,t,s}=G_{bp}(V_{b,t,s}^{2}-V_{p,t,s}^{2})/2-B_{bp}\delta_{bp,t,s}+P_{bp}^{L},\forall t\in T,\ \forall b\in N_{bus},\forall s\in S \tag{6}$$

$$Q_{bp,t,s}=-B_{bp}(V_{b,t,s}^{2}-V_{p,t,s}^{2})/2-G_{bp}\delta_{bp,t,s}+Q_{bp}^{L},\forall t\in T,\ \forall b\in N_{bus},\forall s\in S \tag{7}$$

$$-T_{ij}^{max}\le P_{t}^{e}\le T_{ij}^{max},\ \forall t\in T \tag{8}$$

$$GS_{g,t,s}=GS_{g,t-1,s}-P_{g,t,s}\Delta t\ \forall t\in T-\{1\},\forall g\in N_{g} \tag{9}$$

$$GS_{g}^{min}\le GS_{b,t,s}\le GS_{g}^{Ini},\forall t\in T,\forall g\in N_{g},\forall s\in S \tag{10}$$

Eqs. (11)–(12) represent the operational constraints of voltage limit and line capacity, while Eqs. (13)–(14) correspond to the power generation limit of conventional generators. These constraints capture the technical features of MG operations and ensure the accuracy of obtained solutions. Note that $V_{b,t,s}^{2}$ will be treated as a variable in this linearized OPF. Constraint (12) is quadratic and defines a convex region, which can be linearized via the piecewise linearization method suggested in [38]. As such, the typical non-linear AC OPF is linearized into a MILP formulation and can be solved efficiently via commercial softwares (e.g., CPLEX and GUROBI) [39]. Compared with EMS or DC OPF, this linearization method takes reactive power and voltage into account. Compared with linearized Distflow, this approach can be utilized for both meshed and radial networks and effectively capture power losses through loss factors. However, there still exists a risk for the linearized OPF to obtain solutions that do not satisfy the original power flow equations [40]; hence, it is necessary to verify the practical feasibility of obtained solutions through a detailed non-linear AC OPF algorithm, which is introduced in the third stage.

$$(V^{min})^{2}\le V_{b,t,s}^{2}\le(V^{max})^{2},\forall t\in T,\forall b\in N_{bus},\forall s\in S \tag{11}$$

$$P_{bp,t,s}^{2}+Q_{bp,t,s}^{2}\le S_{bp}^{lim},\forall t\in T,\forall bp\in N_{br},\forall s\in S \tag{12}$$

$$P_{g}^{min}\le P_{g,t,s}\le P_{g}^{max},\forall t\in T,\forall g\in N_{g},\forall s\in S \tag{13}$$

$$Q_{g}^{min}\le Q_{g,t,s}\le Q_{g}^{max},\forall t\in T,\forall g\in N_{g},\forall s\in S \tag{14}$$

MESS-related constraints are shown in Eqs. (15)–(20). It is assumed that MESSs can move between different buses within each MG. Inequalities (15) and (16) refer to the limits of charging and discharging power for MESS k. Integer variable $u^{c}(b,k,t)$ and $u^{d}(b,k,t)$ correspond to charging and discharging decisions of MESS k in bus b at time step t. Constraint (17) ensures that power charging and discharging cannot occur simultaneously, while MESS k can only be connected with one bus at each time step. Note that $u^{c}(b,k,t)=0$ and $u^{d}(b,k,t)=0$ mean that the MESS k does not connect with bus b at time step t and vice versa. Constraint (18) corresponds to the transportation of MESS k within an MG, where $D(b,p)$ represents the traveling time of MESS k from bus b to bus p [41]. Inequality (19) gives the minimum and maximum energy storage limits of MESS k, while constraint (20) introduces the dependence of energy storage level at each time interval with the previous time step.

$$0\le P_{b,k,t}^{mes,c}\le u_{b,k,t}^{c}\cdot P_{k}^{max},\forall t\in T,\forall b\in N_{bus},\forall k\in N_{mes} \tag{15}$$

$$0\le P_{b,k,t}^{mes,d}\le u_{b,k,t}^{d}\cdot P_{k}^{max},\forall t\in T,\forall b\in N_{bus},\forall k\in N_{mes} \tag{16}$$

$$\sum_{b\in N_{bus}}u_{b,k,t}^{c}+u_{b,k,t}^{d}\le 1,\forall t\in T,\forall k\in N_{mes} \tag{17}$$

$$[u_{b,k,t}^{c}+u_{b,k,t}^{d}]-[u_{b,k,t+1}^{c}+u_{b,k,t+1}^{d}]\le 1-[u_{p,k,t+h}^{c}+u_{p,k,t+h}^{d}],\quad \forall t\in T-\{1\},\ \forall k\in N_{mes},b\ne p\in N_{bus},h\in[1,\dots,\min(D_{bp},T-t)] \tag{18}$$

$$ES_{k}^{min}\le ES_{k,t}\le ES_{k}^{max},\forall t\in T,\forall k\in N_{mes} \tag{19}$$

$$ES_{k,t}=ES_{k,t-1}+(\eta^{c}\sum_{b\in N_{bus}}P_{b,k,t}^{mes,c}-\eta_{d}\sum_{b\in N_{bus}}P_{b,k,t}^{mes,d})\Delta t,\ \forall t\in T-\{1\},\quad \forall k\in N_{mes} \tag{20}$$

3.2. Stage 2 — Consensus algorithm for power exchange

After extreme events, the communication between the central controller of utility grid and the local controller of each MG may be unavailable; nevertheless, part of the local connection among nearby MGs may still be reliable, which renders the application of distributed control approaches valid for the decision making of power exchange among nearby MGs under emergency situations. In this paper, a consensus-based algorithm is employed to optimize the power sharing results among interconnected MGs. Note that consensus algorithms have recently gained popularity in power dispatch problems because of their fast convergence and stability [22]. Given the consideration of resilience, the incremental cost of load shedding $\lambda_{i,t}$ of each MG i constitutes the consensus variables. Each MG estimates the values of their power shortage through the first stage and then updates these estimates by exchanging information with neighboring MGs. The communication network of this MG cluster can be represented by matrices W and E, which have the following properties [22]:

- W is a row-stochastic matrix (summation of row entries is equal to one), while E is a column-stochastic matrix and $E=W^{T}$.
- $W_{i,j}>0$ means that MG i is connected to MG j.
- The values of W and E can be free to choose, which will not influence the convergence rate.

Specifically, the suggested consensus algorithm involves a four-step iterative process, which can be outlined below:

Step 1 (Initialization) Using the results from the first stage, the power shortage/surplus and power mismatches estimated by MG i are noted as below. Note that $P_{i,t}^{sho}$ and $P_{i,t}^{sur}$ will be derived from P^{e} of each MG.

$$P_{i,t}^{sho},P_{i,t}^{sur},P_{i,t}^{mis},\forall i\in M,\forall t\in T \tag{21}$$

Regarding MG i, the power obtained from connected MGs is initialized as $P_{i,t}^{ob,0}$, where 0 means the first iteration. Note that $P_{i,t}^{ob,0}$ can be initialized as any feasible values [22]. Additionally, the total available

or required power P_t^{total} in the local network and the power mismatch $P_{i,t}^{mis,0}$ can be calculated as follows:

$$P_t^{total} = \min[\sum_{i\in M} P_{i,t}^{sur}, \sum_{i\in M} P_{i,t}^{sho}] \tag{22}$$

$$P_{i,t}^{mis,0} = P_t^{total}/M - P_{i,t}^{ob,0} \tag{23}$$

Step 2 (Consensus variable update) At each iteration k, each MG i updates $\lambda_{i,t}$ and $P_{i,t}^{ob}$ based on the values of consensus variables obtained from connected MGs, which can be calculated as follows (η is the learning gain constant):

$$\lambda_{i,t}^{k+1} = \sum_{j\in M} W_{i,j}\lambda_{j,t}^{k} + \eta P_{i,t}^{mis,k} \tag{24}$$

$$P_{i,t}^{ob,k+1} = (\lambda_{i,t}^{k+1} - \beta_i)/(2\alpha_i) \tag{25}$$

Step 3 (Power mismatch update) Each MG i updates its power mismatch estimates based on (i) its neighboring MGs' estimates and (ii) a correction term which is given by the difference between its optimal responses at the two most recent iterations.

$$P_{i,t}^{mis,k+1} = \sum_{j\in M} E_{i,j}P_{j,t}^{mis,k} - (P_{i,t}^{ob,k+1} - P_{i,t}^{ob,k}) \tag{26}$$

Step 4 (Convergence check) This process is repeated until the mismatch is within the acceptable range, i.e. less than ϵ. This condition assures the convergence of the algorithm.

$$P_{i,t}^{mis} \le \epsilon, \forall i \in M \tag{27}$$

3.3. Stage 3 — Detailed non-linear AC OPF for feasible solutions

As mentioned before, MG operations can be much closer to stability limits due to the high-impact nature of extreme events, which leads to the necessity to ensure no violation of technical constraints relating to voltage, angle, and power losses. Solutions obtained from the linearized AC OPF algorithm in the first stage may not satisfy classical non-linear power flow equations, even though computing efficiency can be guaranteed. As such, a detailed non-linear AC OPF algorithm capturing all the technical constraints is employed in this stage to verify the feasibility of final optimization results and ensure no violations of technical constraints for accurate decision making. Specifically, the AC OPF algorithm can be formulated as a non-linear programming (NLP) problem without any integer variables, since the routing and scheduling decisions of MESSs at the current time step are obtained from the first stage. Additionally, the results of power exchange capturing the influence of future time slots are obtained from the second stage via the consensus algorithm. Furthermore, the non-linear AC OPF algorithm can be solved for each time step in a deterministic manner, which ensures computing efficiency. The objective function in the third stage can be found in (28), aiming to minimize the load shedding cost for the current time step t.

$$F_3 = \sum_{b\in L_{bus}} c_b^{ls} P_{b,t}^{ls} \tag{28}$$

In more detail, the linearized power flow equations (i.e., (4)–(7)) are replaced by the typically non-linear power flow equations, which can be found in (29)–(30). The quadratic constraint (12) related to line capacity can directly be included in the model for accurate optimization results without any linearization technique. Constraints relating to voltage and line capacity limits (11)–(12), generation limits (9)–(10) and (13)–(14), and power balance equations (2)–(3), will be the same as those in the first stage, while constraints of power exchange limit (8) and MESS routing and scheduling characteristics (15)–(20) are not necessary for the third stage. As such, the non-linear model of a detailed AC OPF is formulated, which is used for the verification of decisions on power exchange as well as MESS routing and scheduling. To ensure that solutions with good quality are found, a non-linear solver called 'IPOPT' is utilized to solve this operational problem [42].

$$P_{b,t}^{ex} = \sum_{p\in N_{bus}} V_{b,t}V_{p,t}(G_{bp}cos\delta_{bp,t} + B_{bp}sin\delta_{bp,t}),\ \forall t \in T,\ \forall b \in N_{bus} \tag{29}$$

$$Q_{b,t}^{ex} = \sum_{p\in N_{bus}} V_{b,t}V_{p,t}(G_{bp}sin\delta_{bp,t} - B_{bp}cos\delta_{bp,t}),\ \forall t \in T,\ \forall b \in N_{bus} \tag{30}$$

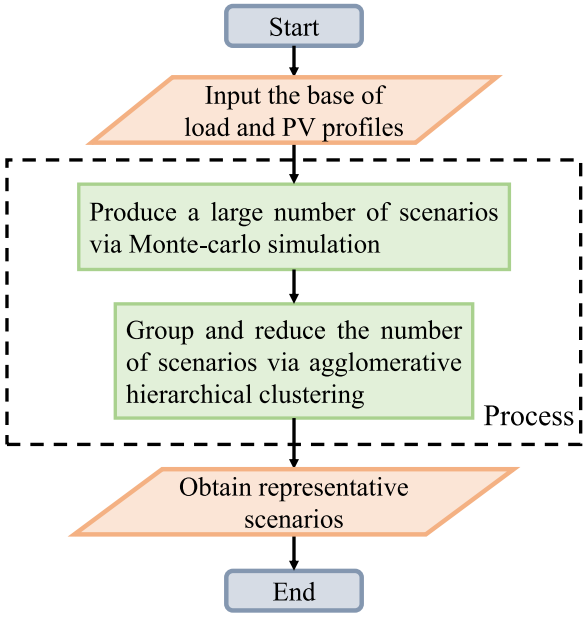

Fig. 3. Uncertainty modeling process of renewable energy sources and load profiles.

3.4. Uncertainty modeling

Uncertainties relating to renewable energy resources (e.g., PVs) and load profiles shall be considered in the proposed rolling optimization framework due to the highly unpredictable nature of extreme events, since accurately updated forecasts over a long rolling horizon are normally unavailable. This paper utilizes a scenario-based stochastic programming approach to capture these uncertainties, including the following two steps:

- Employ Monte-Carlo simulation to initialize a large number of scenarios (e.g., 1000 scenarios) following Beta and normal distribution functions, where PV and load profiles are associated with 5% and 3% errors respectively [35].
- Utilize the agglomerative hierarchical clustering approach (bottom-up structure) with Ward's linkage in the group for scenario reduction [43], while considering an appropriate trade-off between computing time and accuracy.

Finally, an uncertain set containing several scenarios with different probabilities (e.g., 20 scenarios) can be obtained to represent the uncertainties associated with PV and load profiles. The detailed process of this uncertainty modeling approach can be found in Fig. 3.

As one of the most prevalent clustering techniques, hierarchical clustering can formulate a hierarchy of clusters by utilizing a measure of similarity between groups of data points [44]. For a pair of clusters k_1 and k_2, the distance measure d_{k_1,k_2} can be calculated as below:

$$d_{k_1,k_2} = \| \Gamma_{k_l} - \Gamma_{k_2} \|_2 \sqrt{2n_{k_1}n_{k_2}/(n_{k_1} + n_{k_2})}, \tag{31}$$

where n_{k_1} and n_{k_2} are the numbers of scenarios in clusters k_1 and k_2, Γ_{k_l} and Γ_{k_2} represent the centroids of clusters k_1 and k_2, and $\| \cdot \|_2$ corresponds to the Euclidean distance.

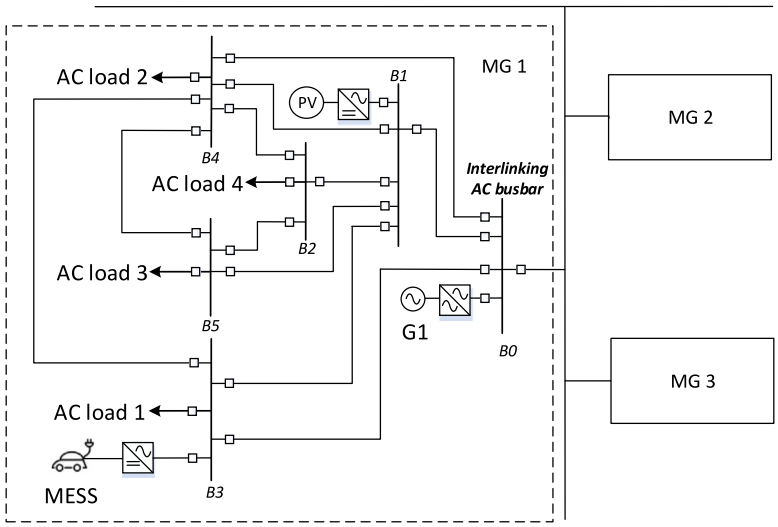

Fig. 4. Network structure of the MG cluster utilized in case studies.

After obtaining these clusters, the medoid point of each cluster is selected to represent one of the final scenarios. Given the initial scenarios have the same probability of occurrence, the weight of each cluster (i.e., the occurrence probability of each final scenario) can be calculated as the ratio of the number of initial scenarios that belong to the cluster and the number of total scenarios [43].

4. Case studies

The stochastic distributed control approach described in the previous section has been applied to the networked MGs illustrated in Fig. 4; note that these MGs switch into islanded mode after extreme events and connect with each other for power sharing. Each MG includes a conventional generator (e.g., diesel generators), a PV, and a MESS as energy resources. Solar irradiation and load profiles utilized in the following case studies are illustrated in Fig. 5, where the data are extracted from [45]. Conventional generators in these three MG have capacities of 150 kW, 350 kW, and 100 kW, respectively. As far as the MESSs are concerned, each MG includes one MESS containing a typical low-energy and low-power battery (i.e., 50 kW/200 kWh), which is initially deployed at bus 3 of each MG. Through the extensive analysis of the following case studies, the paper addresses fundamental modeling challenges pertaining to the distributed operation of networked MGs with mobile units. All case studies have been run on an Intel i7-8700u processor using 8 GB RAM.

As mentioned before, the key focus should be on critical load restoration during extreme events; hence, the discrimination of critical and non-critical loads is captured in the following case studies. For instance, critical loads could be lights and lift motors in a small-scale MG, while non-critical loads might be kitchen and toilet appliances [46]. This paper assumes that around 30% of the loads are critical with high curtailment costs, while other loads are non-critical with relatively low curtailment costs. Specifically, critical loads are located at bus 3 of each MG in the cluster, while non-critical loads are located at bus 4 and bus 5 of each MG. Regarding uncertainty modeling, a total of 20 scenarios are generated to represent uncertainties relating to RESs and load profiles. The sets of uncertainties in MG 1 are illustrated in Fig. 6. Additionally, the network status after the event (i.e., contingencies) can be found in Table 1. It is worth noting that this paper assumes severe damage in each MG to mimic the high-impact nature of extreme events.

Table 1
Contingencies in the investigated MG cluster.

	MG 1	MG 2	MG 3
Line outages	line 1–3, 3–4	line 2–4, 2–5, 3–4	line 1–5, 3–4, 4–5

Table 2
Critical and total load shedding in the MG cluster under the proposed distributed control approach.

	Critical load shedding (kW)	Total load shedding (kW)
MG 1	1.36	210.78
MG 2	0	155.92
MG 3	0	1392.86

4.1. Case study I: Results of MESS routing and distributed control

In this subsection, optimization results using the suggested distributed control are demonstrated, where Table 2 illustrates the results of load shedding in each MG including both critical and non-critical load shedding. Note that there is only minimal critical load shedding in MG 1, while other MGs have no critical load shedding. Table 1 shows that line outages happening in MG 1 are both related to bus 3, which is connected with critical loads, while MG 2 and MG 3 only have one faulted line connected with bus 3; hence, critical load shedding is indeed expected in MG 1. As shown in Fig. 5, MG 3 has the highest load level and the relatively low generator rating that leads to the largest total load shedding, while MG 2 has the lowest total load shedding due to the largest generator rating. Load shedding on an hourly basis is illustrated in Fig. 7. More intensive load shedding is caused in networked MGs during the period of peak load level (e.g., 10–15 h).

The time-coupled routing behaviors of MESSs in each MG can be found in Table 3. In general, MESSs travel back and forth between bus 0 connecting the generator and other buses connecting loads towards load restoration. Note that the suggested rolling optimization can consider the mobility and flexibility of MESSs during a long scheduling horizon, compared with hourly resolutions which cannot capture the flexibility of MESSs. Fig. 8 corresponds to the charging and discharging characteristics of MESSs in each MG. To further exhibit the merits of MESSs on load restoration, a comparative case study between MESSs and ESSs is suggested in this subsection, where both MESSs and ESSs have the same power capacities and energy capacities. Table 4 reports the optimal results of using MESSs and ESSs for resilience enhancement respectively. It can be found that MESSs obtain much less total load

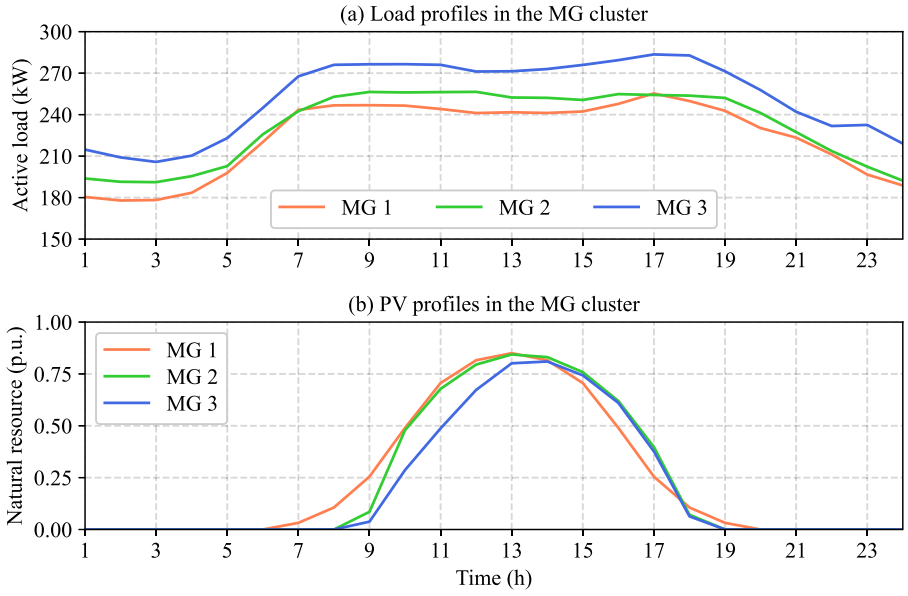

Fig. 5. Load and PV profiles in the MG cluster.

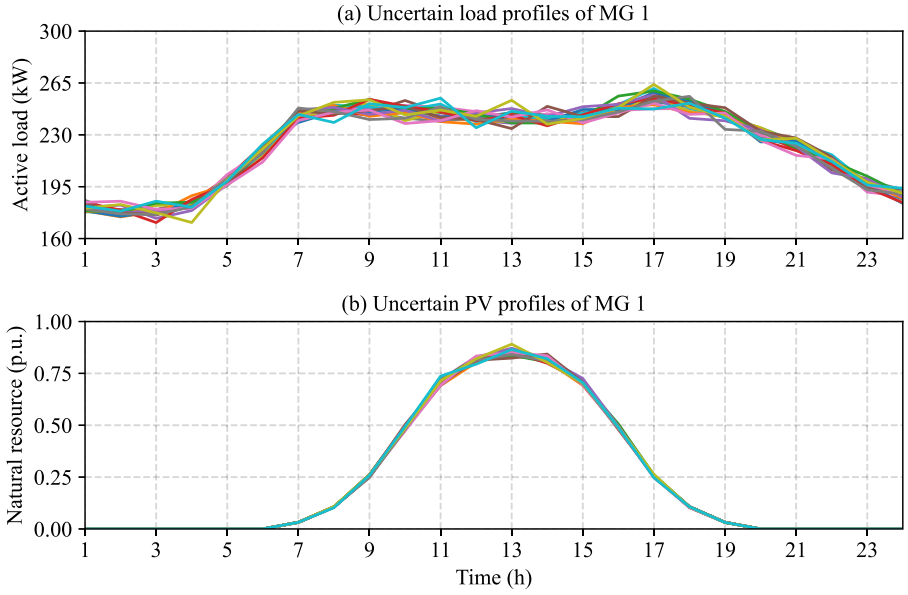

Fig. 6. Uncertainty sets of load and PV profiles in MG 1.

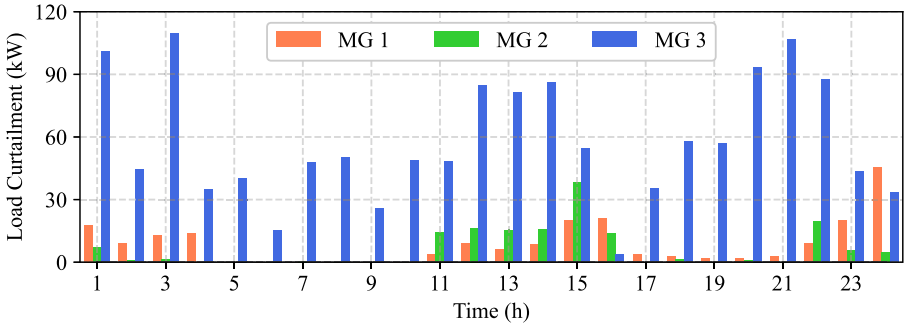

Fig. 7. Hourly load curtailment in the MG cluster under the proposed distributed control approach.

Table 3
MESS routing behaviors inside each MG under the proposed distributed control approach.

MGs	Time (h)																							
	0	1	2	3	4	5	6	7	8	9	10	11	12	13	14	15	16	17	18	19	20	21	22	23
MG 1	3	3	3	T	5	5	5	5	5	5	T	0	0	0	0	T	5	5	5	5	5	5	T	0
MG 2	3	T	0	T	5	5	5	5	5	5	T	0	0	0	0	T	5	5	5	5	5	5	T	0
MG 3	3	T	0	0	T	5	5	5	5	T	0	0	0	0	T	5	5	5	5	T	0	0	T	5

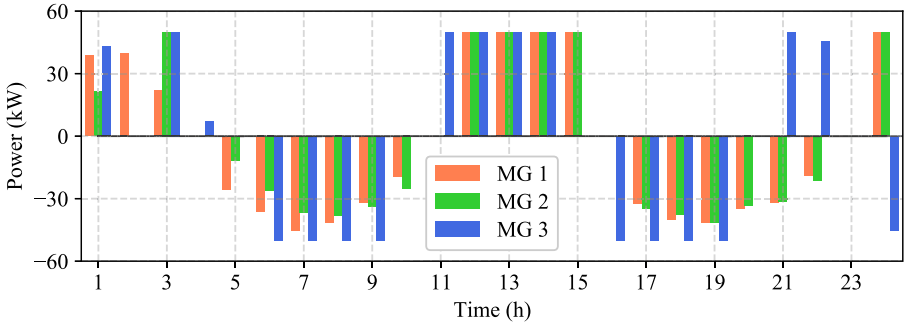

Fig. 8. Charging and discharging characteristics of MESSs in the MG cluster.

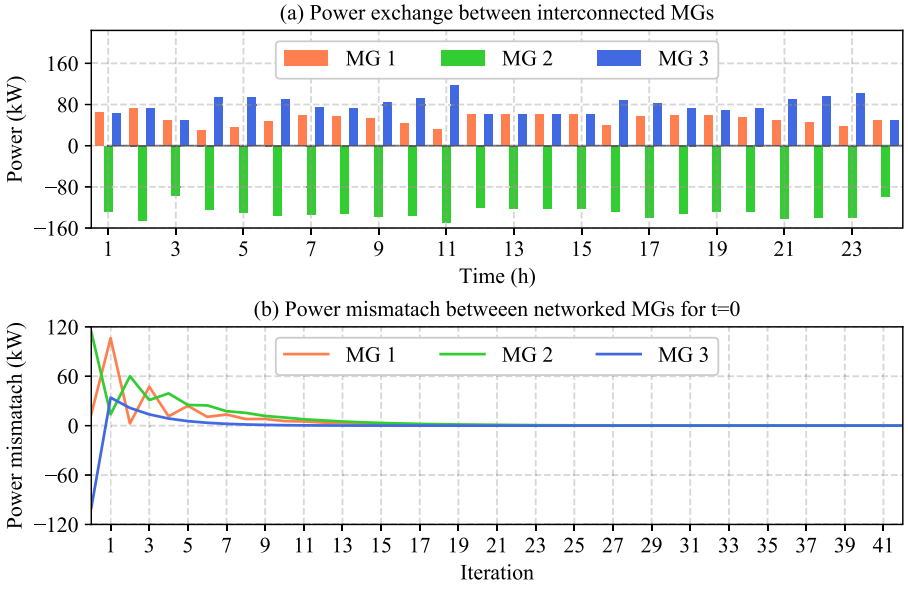

Fig. 9. Power exchange results and the iteration of power mismatch for $t = 0$ under the suggested distributed control approach.

Table 4
Comparison between MESSs and ESSs including load shedding quantities and costs.

	Critical load shedding (kW)	Total load shedding (kW)	Load shedding cost (k£)
MESSs	1.36	1759.56	264.07
ESSs	56.73	2257.04	344.23

shedding cost due to the mobility merit. Additionally, much critical load shedding is avoided when MESSs are employed for resilience enhancement.

Fig. 9(a) illustrates the power exchange results from the consensus algorithm, while Fig. 9(b) exhibits the iteration of power mismatch among these MGs for $t = 0$. After extreme events, all MGs switch into islanded mode and the generator in MG 2 has the largest capacity, which triggers the power flow from MG 2 to the other two MGs. Additionally, Fig. 5(a) shows that MG 3 has the highest load level, therefore receives significantly more power from MG 2 than MG 1 does.

The advantage of the detailed non-linear AC OPF algorithm can be found in Fig. 10. Voltage profiles of bus 3 in all three MGs are restricted within the range of voltage limits (e.g., 0.9–1.1 p.u.). This is important, as typical energy management systems found in the literature would not capture the voltage constraints; this would lead to violation of technical requirements. Even though the voltage constraint of the suggested non-linear OPF may negatively impact the operational cost for keeping voltages stable, it can capture realistic optimization results and ensure secure MG operations; a highly important feature as we move in broad decentralization.

4.2. Case study II: Effect of limited generation resources

The above case study assumes that generation resources are unlimited, which is the reason that there is consistently power sharing between MGs as shown in Fig. 9(a) and there is almost no critical load shedding in each MG. However, as mentioned before, the generation

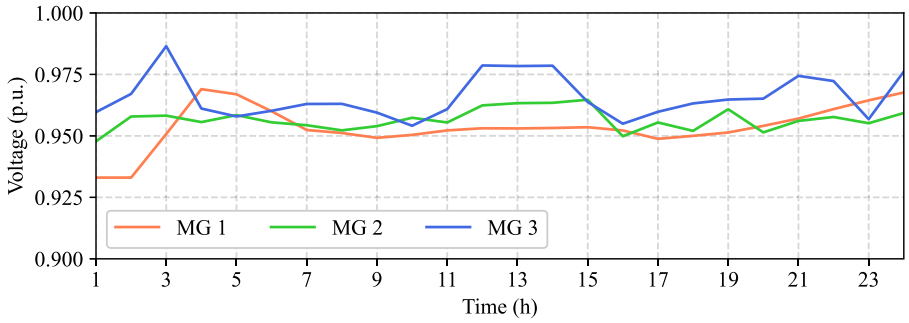

Fig. 10. Voltage profiles of bus 3 in the MG cluster.

Table 5
Critical and total load shedding in the MG cluster under limited generation resources.

	Critical load shedding (kW)	Total load shedding (kW)
MG 1	56.18	580.79
MG 2	0	107.09
MG 3	9.78	1962.20

Table 6
Comparison of load shedding costs and computing time under different rolling horizons.

	Load shedding cost (k£)	Computing time for one step (s)
5 h	283.02	0.76
15 h	253.20	6.67
24 h	264.07	29.04

resources can be limited during extreme events, because of the potential disruption of the energy supply chain. In this case study, the effect of limited generation resources on optimal results is exhibited, where it is assumed that MG 1–3 only have 3500 kWh, 10000 kWh, and 5000 kWh available resources during the event, respectively.

Results of final load shedding of the MG cluster can be found in Table 5. It is shown that critical load shedding is caused in MG 1 and MG 3, while total load shedding in every MG has significantly increased compared with the results in the case study above. The reason can be found in Fig. 11(a), which exhibits the final power sharing results among MGs. In the first 12 hours, there is a large amount of power supply from MG 2 to other MGs. However, after this time period, the intensity and frequency of power sharing among MGs reduce a lot, leading to much larger load shedding in MG 1 and MG 3. This is because the suggested stochastic distributed control approach based on rolling optimization always considers a complete scheduling horizon (e.g., the next 24 hours). As such, after around 12 hours, MG 2 tends to distribute its generation resources for its own future usage (i.e., reducing load shedding) rather than using them for power sharing, which causes a reduced amount of power sharing. Fig. 11(b) illustrates that there is much more load shedding caused in MG 1 and MG 3 in the last 10 hours.

4.3. Case study III: Non-cooperative behavior of MGs

The main difference between networked MG systems under centralized control and distributed control is the protection of MG privacy and localized decision making. As suggested in [19], MGs may try to manipulate certain operating limits to further improve their own benefits (e.g., reducing operational cost), which is categorized as non-cooperative or dishonest behavior. Especially during extreme events, it may be reasonable for a certain MG to maintain higher levels of energy under its own territory for self-protection by reporting wrong values of power exchange limits.

The three-stage model developed in this paper can simulate the non-cooperative behaviors of MGs via a simple method explained hereafter. Let us assume that MG 2 may tend to reduce power export to the other MGs, since it has a conventional generator with a large rating and may be reluctant to share more energy with other MGs during an event. In this case, MG 2 may choose to report lower values of power exchange limits T_{ij}^{max} (e.g., from 150 kW to 100 kW or 50 kW), which will have a significant influence on optimal results of power exchange among MGs and final results of load shedding cost. As expected, Fig. 12 illustrates that load shedding cost has largely increased when MG 2 reduces its power exchange limitation from 150 kW to 100 kW or 50 kW. Fig. 13 corresponds to the power exchange results under the non-cooperative behavior of MG 2, which exhibits that less power can be imported into MG 1 and MG 3.

5. Discussion

5.1. Sensitivity analysis investigating the influence of different rolling horizons

This section illustrates, through an appropriate sensitivity analysis, the influence of different rolling horizons on optimal results of the proposed three-stage distributed control scheme; refer to Table 6. On one hand, selecting a very short rolling horizon (e.g., 5 h) may not sufficiently capture information regarding future uncertainties, which can lead to increased load shedding costs. On the other hand, if a long rolling horizon (e.g., 24 h) is selected, MGs may be convinced to share their resources conservatively which can cause slightly more load shedding, compared with a slightly shorter horizon (e.g., 15 h). All three scenarios shown in Table 6 can be efficiently solved on an hourly basis via commercial softwares, while a longer scheduling horizon can lead to longer computing time; note the exponential increase in computing time. Additionally, it shall be mentioned that the selection of the rolling horizon is empirical and shall be appropriately decided according to realistic scenarios. For instance, a longer rolling horizon could be used to better capture future uncertainties, if the event was to last for a long period (e.g., several days).

5.2. A comparison between different control approaches

To further verify the advantages of the proposed three-stage stochastic distributed control approach on timely load restoration, a detailed comparison among different methods are conducted in this subsection, including two benchmark methods: (1) a deterministic time-coupled centralized control approach without rolling optimization, assuming perfect information of RESs and load profiles; (2) a stochastic centralized control approach within the rolling optimization framework (24 hour rolling horizon), capturing the uncertainties associated with RESs and load profiles.

Table 7 summarizes the load shedding cost and the computing time of three different control approaches. It can be observed that the deterministic centralized control approach achieves the lowest load

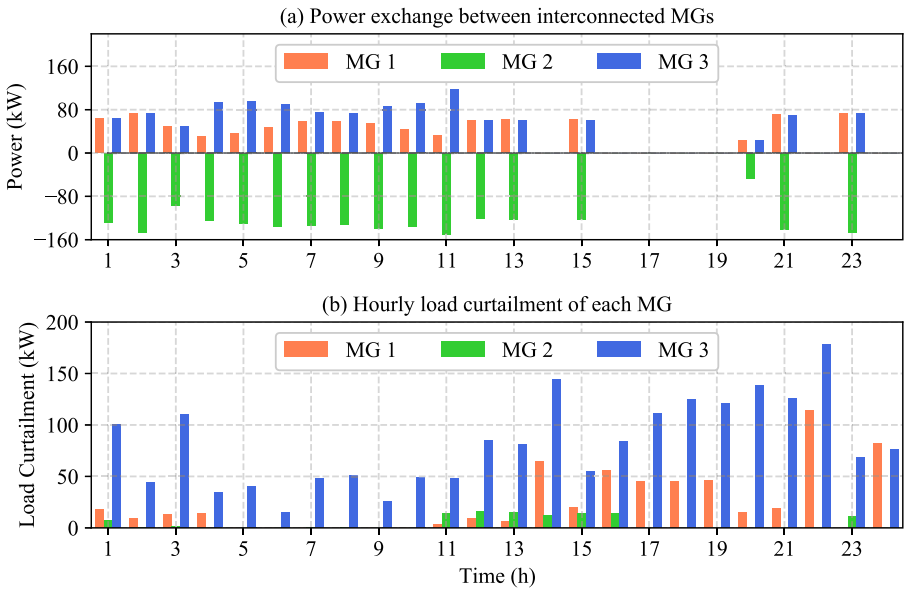

Fig. 11. Power exchange among MGs and hourly load curtailment in the MG cluster under limited generation resources.

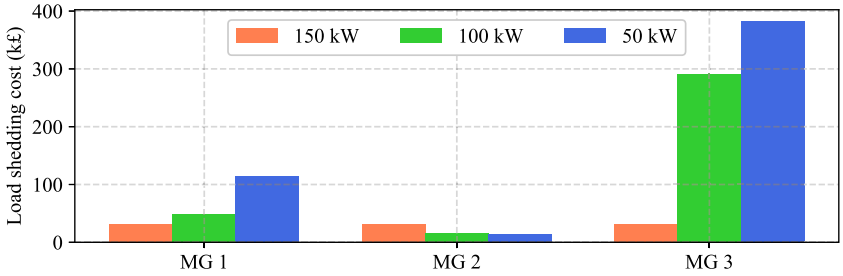

Fig. 12. Load shedding cost under the non-cooperative behavior of MG 2.

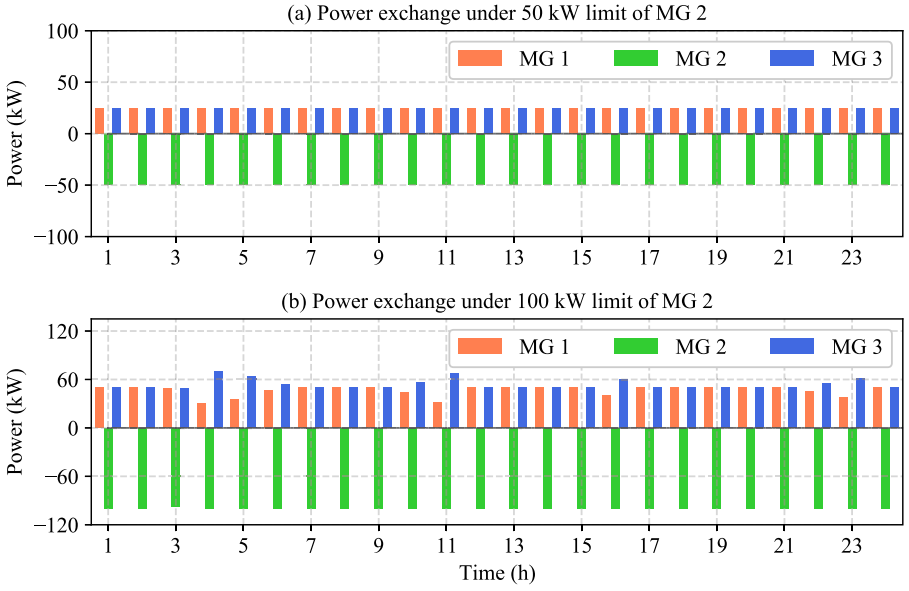

Fig. 13. Power exchange results among MGs: (a) under 50 kW exchange limit of MG 2, (b) under 100 kW exchange limit of MG 2.

shedding cost because of the assumption of perfect uncertainty information; nevertheless, this assumption is normally unrealistic. However, it can also be found that the load shedding cost (264.07 k£) obtained from the proposed distributed control approach is very close to two centralized control approaches, i.e., 5.71% higher than deterministic centralized control (249.81 k£) and 2.30% higher than stochastic centralized control (258.14 k£). Regarding the computing time, it can be observed from Table 7 that the proposed stochastic distributed control approach obtains the shortest computing time 29.04 s, while deterministic centralized control and stochastic centralized control obtain

Table 7
Comparison of load shedding costs and computing time under three different control approaches.

	Load shedding cost (k£)	Computing time for one step (s)
Deterministic centralized control	249.81	150.32
Stochastic centralized control	258.14	3102.33
Proposed distributed control	264.07	29.04

150.32 s and 3102.33 s respectively. The reason is that MG operations in the first and third stages of the suggested three-stage approach are formulated in a decentralized manner and then run in parallel, which largely reduces the computational burden. It is worth noting that achieving fast response and timely load restoration is important for the resilience enhancement of networked MGs due to the high-impact and unpredictable nature of extreme events. This comparative analysis demonstrates the merits of the proposed approach in terms of load restoration and computing efficiency, which becomes significantly important in energy systems with high penetration of DERs that should be managed as close to real time as possible.

6. Conclusions

In this paper, a three-stage stochastic distributed control approach based on rolling optimization is suggested to enhance the resilience of networked MGs with MESSs. Specifically, a stochastic linearized AC OPF algorithm is utilized in the first stage to capture the influence of uncertainties relating to renewable generation resources and load profiles as well as the flexibility of MESSs and power sharing among MGs. A consensus-based algorithm is employed in the second stage to obtain the final results of power sharing among interconnected MGs, and finally a detailed non-linear AC OPF algorithm constitutes the third stage towards capturing technical constraints regarding stability properties and obtaining accurate optimization results. Overall, the suggested three-stage approach provides benefits over other distributed control approaches found in the literature, as it can capture uncertainties, MESS routing and scheduling characteristics as well as ensure computing efficiency. Additionally, this approach can be applied in different networked structures including both radial and meshed networks. Load distinction into critical and non-critical, the limitation of generation resources, and the non-cooperative behaviors of MGs are appropriately considered in case studies to capture realistic scenarios and verify the effectiveness of the suggested three-stage distributed control approach.

In more detail, there are three key findings observed from the case study results: (1) the proposed stochastic distributed control approach can effectively avoid critical load shedding while ensuring a fast response to potential extreme events; (2) MESSs can coordinate with the MG cluster via their routing and scheduling characteristics for more effective load restoration; (3) the potential risks of limited generation resources and non-cooperative behaviors of MGs can lead to more conservative power exchange behaviors and then cause more load shedding. Future work may focus on the resilience-oriented coordination problem of different mobile power resources in the context of decentralized networked MGs, including MESSs, mobile emergency generations, repair crews, and even electric vehicles. It may also be interesting to develop a more comprehensive resilience-oriented operation model for networked MGs, involving the preventive stage, corrective stage, and restoration stage.

CRediT authorship contribution statement

Y. Wang: Conceptualization, Validation, Writing – original draft, Writing – review & editing, Visualization. **A. Oulis Rousis:** Writing – review & editing, Validation, Visualization. **D. Qiu:** Writing – review & editing, Validation, Visualization. **G. Strbac:** Resources, Funding acquisition, Supervision.

Declaration of competing interest

The authors declare that they have no known competing financial interests or personal relationships that could have appeared to influence the work reported in this paper.

Data availability

No data was used for the research described in the article.

Acknowledgments

This work was supported by two UK EPSRC projects: ‘Integrated Development of Low-Carbon Energy Systems (IDLES): A Whole-System Paradigm for Creating a National Strategy’ (project code: EP/R045518/1) and ‘Technology Transformation to Support Flexible and Resilient Local Energy Systems’ (project code: EP/T021780/1), and one Horizon Europe project: ‘Reliability, Resilience and Defense technology for the griD’ (Grant agreement ID: 101075714) as well as the National Natural Science Foundation of China under Grants 62103371, 52161135201, U20A20159, 62061130220.

References

[1] Bie Z, Lin Y, Li G, Li F. Battling the extreme: A study on the power system resilience. Proc IEEE 2017;105(7):1253–66.
[2] Aldarajee AH, Hosseinian SH, Vahidi B, Dehghan S. A coordinated planner-disaster-risk-averse-planner investment model for enhancing the resilience of integrated electric power and natural gas networks. Int J Electr Power Energy Syst 2020;119:105948.
[3] Zhu J, Yuan Y, Wang W. An exact microgrid formation model for load restoration in resilient distribution system. Int J Electr Power Energy Syst 2020;116:105568.
[4] Wang Y, Rousis AO, Strbac G. On microgrids and resilience: A comprehensive review on modeling and operational strategies. Renew Sustain Energy Rev 2020;134:110313.
[5] Strbac G, Hatziargyriou N, Lopes JP, Moreira C, Dimeas A, Papadaskalopoulos D. Microgrids: Enhancing the resilience of the European megagrid. IEEE Power Energy Mag 2015;13(3):35–43.
[6] Li Z, Shahidehpour M, Aminifar F, Alabdulwahab A, Al-Turki Y. Networked microgrids for enhancing the power system resilience. Proc IEEE 2017;105(7):1289–310.
[7] Chen L, Liu W, Shi Q, Lyu X, Bai Y, Zhang S, et al. Prospect theory-based optimal configuration of modular mobile battery energy storage in distribution network considering disaster scenarios. Int J Electr Power Energy Syst 2022;142:108215.
[8] Papari B, Edrington CS, Ghadamyari M, Ansari M, Ozkan G, Chowdhury B. Metrics analysis framework of control and management system for resilient connected community microgrids. IEEE Trans Sustain Energy 2021;13(2):704–14.
[9] Barnes A, Nagarajan H, Yamangil E, Bent R, Backhaus S. Resilient design of large-scale distribution feeders with networked microgrids. Electr Power Syst Res 2019;171:150–7.
[10] Wang Z, Wang J. Self-healing resilient distribution systems based on sectionalization into microgrids. IEEE Trans Power Syst 2015;30(6):3139–49.
[11] Liang Z, Alsafasfeh Q, Su W. Proactive resilient scheduling for networked microgrids with extreme events. IEEE Access 2019;7:112639–52.
[12] Ahmadi SE, Rezaei N. A new isolated renewable based multi microgrid optimal energy management system considering uncertainty and demand response. Int J Electr Power Energy Syst 2020;118:105760.
[13] Bazmohammadi N, Tahsiri A, Anvari-Moghaddam A, Guerrero JM. A hierarchical energy management strategy for interconnected microgrids considering uncertainty. Int J Electr Power Energy Syst 2019;109:597–608.
[14] Wang Y, Rousis AO, Strbac G. A resilience enhancement strategy for networked microgrids incorporating electricity and transport and utilizing a stochastic hierarchical control approach. Sustain Energy Grids Netw 2021;26:100464.
[15] Farzin H, Fotuhi-Firuzabad M, Moeini-Aghtaie M. Enhancing power system resilience through hierarchical outage management in multi-microgrids. IEEE Trans Smart Grid 2016;7(6):2869–79.
[16] Wang J, Lu X. Sustainable and resilient distribution systems with networked microgrids. Proc IEEE 2020;108(2):238–41.
[17] Liu Z, Yi Y, Yang J, Tang W, Zhang Y, Xie X, et al. Optimal planning and operation of dispatchable active power resources for islanded multi-microgrids under decentralised collaborative dispatch framework. IET Gener Transm Distrib 2020;14(3):408–22.

[18] Hussain A, Bui V-H, Kim H-M. A resilient and privacy-preserving energy management strategy for networked microgrids. IEEE Trans Smart Grid 2018;9(3):2127–39.
[19] Arsoon MM, Moghaddas-Tafreshi SM. Peer-to-peer energy bartering for the resilience response enhancement of networked microgrids. Appl Energy 2020;261:114413.
[20] Gao H, Xu S, Liu Y, Wang L, Xiang Y, Liu J. Decentralized optimal operation model for cooperative microgrids considering renewable energy uncertainties. Appl Energy 2020;262:114579.
[21] Nikmehr N. Distributed robust operational optimization of networked microgrids embedded interconnected energy hubs. Energy 2020;199:117440.
[22] Hussain A, Bui V-H, Kim H-M. Resilience-oriented optimal operation of networked hybrid microgrids. IEEE Trans Smart Grid 2017.
[23] Lei S, Chen C, Zhou H, Hou Y. Routing and scheduling of mobile power sources for distribution system resilience enhancement. IEEE Trans Smart Grid 2018.
[24] Lei S, Chen C, Li Y, Hou Y. Resilient disaster recovery logistics of distribution systems: Co-optimize service restoration with repair crew and mobile power source dispatch. IEEE Trans Smart Grid 2019;10(6):6187–202.
[25] Yao S, Wang P, Zhao T. Transportable energy storage for more resilient distribution systems with multiple microgrids. IEEE Trans Smart Grid 2018;10(3):3331–41.
[26] Galvan E, Mandal P, Sang Y. Networked microgrids with roof-top solar PV and battery energy storage to improve distribution grids resilience to natural disasters. Int J Electr Power Energy Syst 2020;123:106239.
[27] Wang Z, Chen B, Wang J, Chen C. Networked microgrids for self-healing power systems. IEEE Trans Smart Grid 2015;7(1):310–9.
[28] Wang Z, Chen B, Wang J, et al. Decentralized energy management system for networked microgrids in grid-connected and islanded modes. IEEE Trans Smart Grid 2015;7(2):1097–105.
[29] Arif A, Wang Z. Networked microgrids for service restoration in resilient distribution systems. IET Gener Transm Distrib 2017;11(14):3612–9.
[30] Wei C, Shen Z, Xiao D, Wang L, Bai X, Chen H. An optimal scheduling strategy for peer-to-peer trading in interconnected microgrids based on RO and Nash bargaining. Appl Energy 2021;295:117024.
[31] Li J, Khodayar ME, Wang J, Zhou B. Data-driven distributionally robust co-optimization of P2P energy trading and network operation for interconnected microgrids. IEEE Trans Smart Grid 2021;12(6):5172–84.
[32] Ding T, Wang Z, Jia W, Chen B, Chen C, Shahidehpour M. Multiperiod distribution system restoration with routing repair crews, mobile electric vehicles, and soft-open-point networked microgrids. IEEE Trans Smart Grid 2020;11(6):4795–808.
[33] Liu Y, Li J, Wu L. Coordinated optimal network reconfiguration and voltage regulator/DER control for unbalanced distribution systems. IEEE Trans Smart Grid 2018;10(3):2912–22.
[34] Li J, Ye Y, Papadaskalopoulos D, Strbac G. Consensus-based coordination of time-shiftable flexible demand. In: 2019 international conference on smart energy systems and technologies. IEEE; 2019, p. 1–6.
[35] Najafi J, Peiravi A, Anvari-Moghaddam A, Guerrero JM. An efficient interactive framework for improving resilience of power-water distribution systems with multiple privately-owned microgrids. Int J Electr Power Energy Syst 2020;116:105550.
[36] Yang Z, Zhong H, Bose A, Zheng T, Xia Q, Kang C. A linearized OPF model with reactive power and voltage magnitude: A pathway to improve the MW-only DC OPF. IEEE Trans Power Syst 2017;33(2):1734–45.
[37] Gao H, Chen Y, Xu Y, Liu C-C. Resilience-oriented critical load restoration using microgrids in distribution systems. IEEE Trans Smart Grid 2016;7(6):2837–48.
[38] Yang Z, Zhong H, Xia Q, Bose A, Kang C. Optimal power flow based on successive linear approximation of power flow equations. IET Gener Transm Distrib 2016;10(14):3654–62.
[39] Kronqvist J, Bernal DE, Lundell A, Grossmann IE. A review and comparison of solvers for convex MINLP. Opt Eng 2019;20(2):397–455.
[40] Yang Z, Zhong H, Xia Q, Kang C. Fundamental review of the OPF problem: Challenges, solutions, and state-of-the-art algorithms. J Energy Eng 2018;144(1):04017075.
[41] Kim J, Dvorkin Y. Enhancing distribution system resilience with mobile energy storage and microgrids. IEEE Trans Smart Grid 2018;10(5):4996–5006.
[42] Wächter A, Biegler LT. On the implementation of an interior-point filter line-search algorithm for large-scale nonlinear programming. Math Program 2006;106(1):25–57.
[43] Sun M, Teng F, Zhang X, Strbac G, Pudjianto D. Data-driven representative day selection for investment decisions: A cost-oriented approach. IEEE Trans Power Syst 2019;34(4):2925–36.
[44] Johnson SC. Hierarchical clustering schemes. Psychometrika 1967;32(3):241–54.
[45] Zhang X, Strbac G, Shah N, Teng F, Pudjianto D. Whole-system assessment of the benefits of integrated electricity and heat system. IEEE Trans Smart Grid 2018;10(1):1132–45.
[46] Rousis AO, Konstantelos I, Strbac G. A planning model for a hybrid ac cdc microgrid using a novel GA/AC OPF algorithm. IEEE Trans Power Syst 2020;35(1):227–37.